

Microwave metathetic approach for the synthesis and characterization of ZnCr_2O_4

Purnendu Parhi, V. Manivannan*

Department of Mechanical Engineering, 1374 Campus Delivery, Colorado State University, Fort Collins, CO 80523, USA

Received 16 July 2007; received in revised form 26 October 2007; accepted 2 November 2007

Available online 31 December 2007

Abstract

A novel way to synthesize technologically important ZnCr_2O_4 by microwave metathetic approach using simple precursors such as ZnCl_2 and $\text{Na}_2\text{Cr}_2\text{O}_7$ is described. A proof for the reaction proceeding via metathetic route has been clearly established by XRD diffraction studies. ZnCr_2O_4 , belonging to the “spinel” class of materials, is characterized by multiple techniques to establish structure–property relationship. The band gap of ZnCr_2O_4 is determined to be 3.4 eV, and the ceramic oxide shows anti-ferromagnetic transition (T_N) at -261.5°C . The substitution of Fe into ZnCr_2O_4 (ZCR) results in Fe replacing Cr.

© 2007 Elsevier Ltd. All rights reserved.

Keywords: Microwave processing; Electron microscopy; Magnetic properties; Spinel; ZnCr_2O_4

1. Introduction

Oxides with “spinel” structure are some of the most studied compounds in solid-state sciences due to interesting physico-chemical properties and found useful in many technological applications such as magnetic materials,¹ super hard materials,² and high-temperature ceramics.³ In particular, zinc chromite (ZnCr_2O_4) ceramic spinels are commonly used as catalytic materials,^{4–6} as humidity sensors^{7–9} and as magnetic material.^{10,11}

ZnCr_2O_4 (ZCR) has been synthesized previously by various methods including mechanical activation,^{12,13} high-temperature solid-state reaction,^{4,14–16} micro-emulsion method,¹⁷ solution method,^{18–20} and spray pyrolysis.²¹ Zinc chromite synthesized by Marinkovic et al. by the spray pyrolysis process has nitrogen as an impurity in the final product.¹² This is due to using nitrates as the starting reactants, resulting in the incorporation of nitrogen into the ceramic material. Thus, it is important to recognize that the proper choice of a precursor is important to obtain a pure product. The same research group employed mechanochemical method to synthesize zinc chromite material, by milling the reactant precursors for 5 h. The yield of the

reaction was $\sim 78\%$ and the reaction time was 5 h. Both the reaction yield and the time towards completion of the product can be improved. The microemulsion method carried out by Niu et al. for the synthesis of ZnCr_2O_4 needs a high calcination temperature.¹⁷ Table 1 gives the synthetic condition employed by different research groups towards the preparation of ceramic ZnCr_2O_4 spinel. Therefore, a convenient method of synthesizing ZCR material that overcomes the above disadvantages and limitations in the above synthesis procedures is needed.

Self-propagating solid-state reactions known as solid-state metathesis (SSM) reactions are solventless reactions that enable the synthesis of a wide range of ceramic materials within a short time of duration. These fast, solid-state reactions take advantage of the reaction enthalpy given out in a specific reaction. In a SSM process, a salt with high lattice energy was formed as a by-product, which provides the driving force for the process.²² The reactions can be initiated by using a different source like a heated filament or flames or by igniting the bulk in a furnace or microwave oven.

SSM reactions are now accepted in the scientific community as a way to synthesize a wide range of materials including metal oxides,^{23–36} carbides,²⁷ borides,²⁸ pnictides,²⁹ and chalcogenides.²²

Using microwave energy to synthesize materials in a convenient and simple way has been recognized, since the method is faster, more economical, and cleaner.³⁰ A variety of inorganic

* Corresponding author. Tel.: +1 970 491 2207; fax: +1 970 491 3827.
E-mail address: mani@engr.colostate.edu (V. Manivannan).

Table 1
Synthetic condition employed by different research groups towards the preparation of ceramic ZnCr₂O₄ spinel

No.	Reactants	Synthetic condition for ZnCr ₂ O ₄	Ref.
1	ZnO and Cr ₂ O ₃	Grinding using a planetary ball mill for time 40–320 min	12
2	ZnO and Cr ₂ O ₃	ZnO and Cr ₂ O ₃ powders in equimolar quantities were mechanically activated by grinding using a high energy ball mill for 0, 40, and 80 min	13
3	ZnO and Cr ₂ O ₃	Synthesis by heating the pellet of ZnO and Cr ₂ O ₃ at 1300 °C for 24 h	14
4	ZnO and Cr ₂ O ₃	Synthesis by a conventional solid-state reaction at the temperature of 900 °C during 4 h	15
5	ZnO and Cr ₂ O ₃	Synthesized by a high-temperature solid reaction	16
6	ZnCrO ₄ and CrO ₃	Synthesized by a high-temperature solid reaction	4
7	Zn(NO ₃) ₂ , Cr(NO ₃) ₂ , C ₁₃ H ₂₇ (OCH ₂ CH ₂) _n OH, C ₆ H ₁₃ OH and C ₇ H ₁₆	Synthesis is done by W/O microemulsion method. The coprecipitate were dried at 80 °C for 24 h, then calcined at 800 °C for 3 h	17
8	Zn(NO ₃) ₂ , Cr(NO ₃) ₂ , and C ₄ H ₄ N ₂ O ₂	Synthesis by solution method heating at 375 °C	18
9	Zn(NO ₃) ₂ , Cr(NO ₃) ₂ , and –[CH ₂ CH(OH)] _n	Synthesis by calcination of precursor powders prepared by evaporation of an aqueous solution of polyvinyl alcohol and metal nitrates at 350–450 °C	19
10	Zinc acetate, Cr(CH ₃ COO) ₂ and (CH ₂ CH ₂) ₄ NOH	Synthesis by coprecipitation from solution of the acetate precursors with tetra-Et ammonium hydroxide	20
11	Zn(NO ₃) ₂ , Cr(NO ₃) ₂	Synthesized by a spray pyrolysis method	21

materials such as chalcogenides,^{31,32} nitrides,^{33,34} complex oxides,³⁵ silicides,³⁶ zeolites,³⁷ etc., have been synthesized using the microwave approach.

We have combined the advantages of microwave synthesis of materials with that of the solid-state metathesis route to produce high-quality ZCR ceramic material in a simple way, similar to the work demonstrated earlier.^{23,24} ZCR synthesized by this procedure is faster, and purer, and has the desired stoichiometry and the overall yield of the reaction is around 90%.

2. Experimental

Na₂Cr₂O₇ and ZnCl₂ obtained from Alfa Aesar, USA were employed for the preparation of ZCR ceramic powder. Preparation of ZCR ceramic powder was carried out by grinding Na₂Cr₂O₇ (0.5 g) and ZnCl₂ (0.228 g) in a molar ratio of 1:1 in a pestle and mortar. The powder was transferred to ceramic crucibles of alumina/porcelain and subjected to microwave energy operating at 2.54 GHz with maximum power of 1100 W. No secondary microwave susceptible materials were used. To determine the SSM reaction final adiabatic temperatures Pyro manufactured calibrated Micro Optical Pyrometer with the capability to measure reaction temperatures up to 3200 °C was used.

The final product was obtained from the reactants after washing them with 50 ml of deionized water three times and acetone. Fe doping into ZCR ceramic was accomplished when a calculated amount of FeCl₂ was added to the precursors during the microwave-mediated metathesis reaction as stated above.

Powder X-ray diffraction (XRD) measurements were carried out using a Scintag X2 diffractometer with Cu K α radiation and a Peltier detector. A scan rate of 1°/min with a step size of 0.02° was employed to obtain the XRD spectra. Fourier transmission infrared transform (FTIR) measurements in the 400–4000 cm⁻¹ range were carried out using Nicolet Magna FTIR equipped with deuterated triglycine sulphate (DTGS) detector. Thermogravimetric analysis (TGA) was performed using weight- and temperature-calibrated TA 2950 instruments.

Scanning electron microscope (SEM) characterization was performed on the JSM-6500F, a field emission system with the in-lens thermal field emission electron gun (TFEG). Diffuse reflectance (DR) spectra was recorded in the wavelength range of 250–2500 nm using a Varian Associates Cary 500 double-beam spectrophotometer equipped with a Praying mantis. X-ray photoelectron spectroscopy (XPS) experiments were performed on a physical electronics 5800 spectrometer. This system has a monochromatic Al K α X-ray source ($h\nu = 1486.6$ eV), hemispherical analyzer, and multichannel detector. A low-energy (30 eV) electron gun was used for charge neutralization on the non-conducting samples. The binding energy (BE) scales for the samples were referenced to the C 1s peak at 284.8 eV.³⁸

3. Results and discussion

Fig. 1 shows the XRD of the product before washing, where the ZnCr₂O₄ phase (marked with #) is present along with NaCl (marked with *). The presence of NaCl confirmed that the reaction has proceeded in a metathetic pathway, as established in the

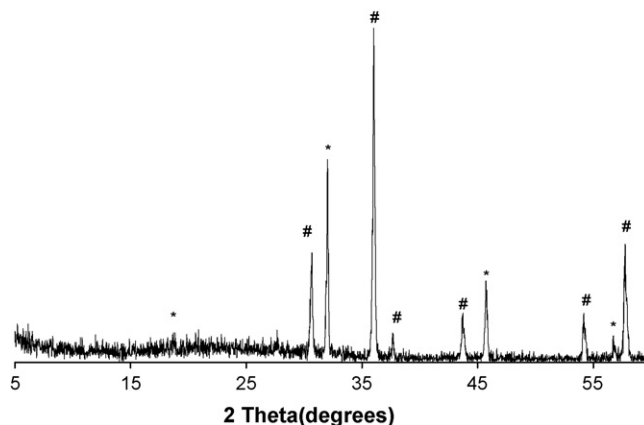


Fig. 1. Powder X-ray diffraction pattern of ZnCr₂O₄ before washing (* shows peaks corresponding to NaCl and # shows peaks corresponding to ZnCr₂O₄).

literature.³⁹ The reaction proceeded is represented as follows:



The high lattice energy of NaCl drives the reaction in the forward direction, enabling the ceramic product formation. NaCl formation, facilitated by the microwave radiation, is the key reason for the formation of ZCR ceramic in a solid state and in a short duration of time. Presence of ZCR peaks along with NaCl peaks in the XRD clears the ambiguity that metathesis reaction enables product formation only in solution or while washing the solids with solvents such as water. The co-existence of the ZCR phase with NaCl thus represents a good example of ceramic materials synthesis by the microwave-mediated solid-state metathetic approach. The final adiabatic temperature of the reaction was measured to be 1310 °C.

XRD of the final product, obtained after washing the reactants thoroughly with water and acetone, is shown in Fig. 2. The intensities of the peaks and the cell parameters obtained clearly confirm that the phases belong to ZnCr_2O_4 and match well with the phase reported in the powder diffraction database.⁴⁰ ZnCr_2O_4 crystallizes in a cubic phase with $a = 8.2800(0) \text{ \AA}$, volume = 567.66 \AA^3 , $Z = 8$, and space group $Fd3m$ (No. 227).

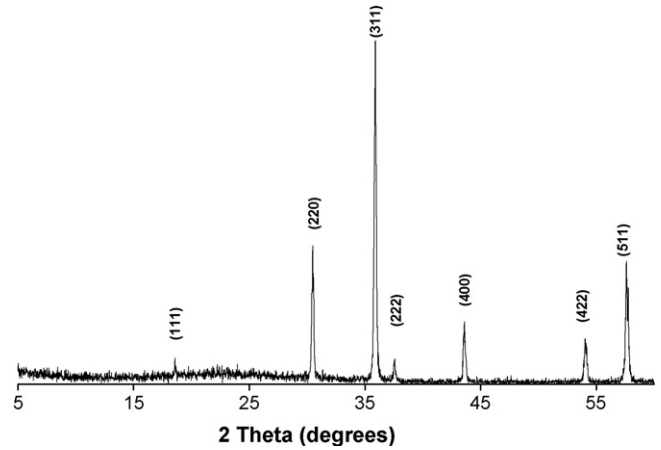


Fig. 2. Powder X-ray diffraction pattern of ZnCr_2O_4 .

The general formula of oxide spinels is AB_2O_4 , where the distribution configuration is represented as $\text{IV}(A_{1-x}B_x)\text{VI}(B_{2-x}A_x)\text{O}_4$. Normal spinels have $x = 0$, whereas inverse spinels have $x = 1$. In the case of normal spinel, the A site is tetrahedrally coordinated and generally occupied by divalent cations (e.g., Mg, Mn, Fe, Ni, Zn). The B site is octahedrally

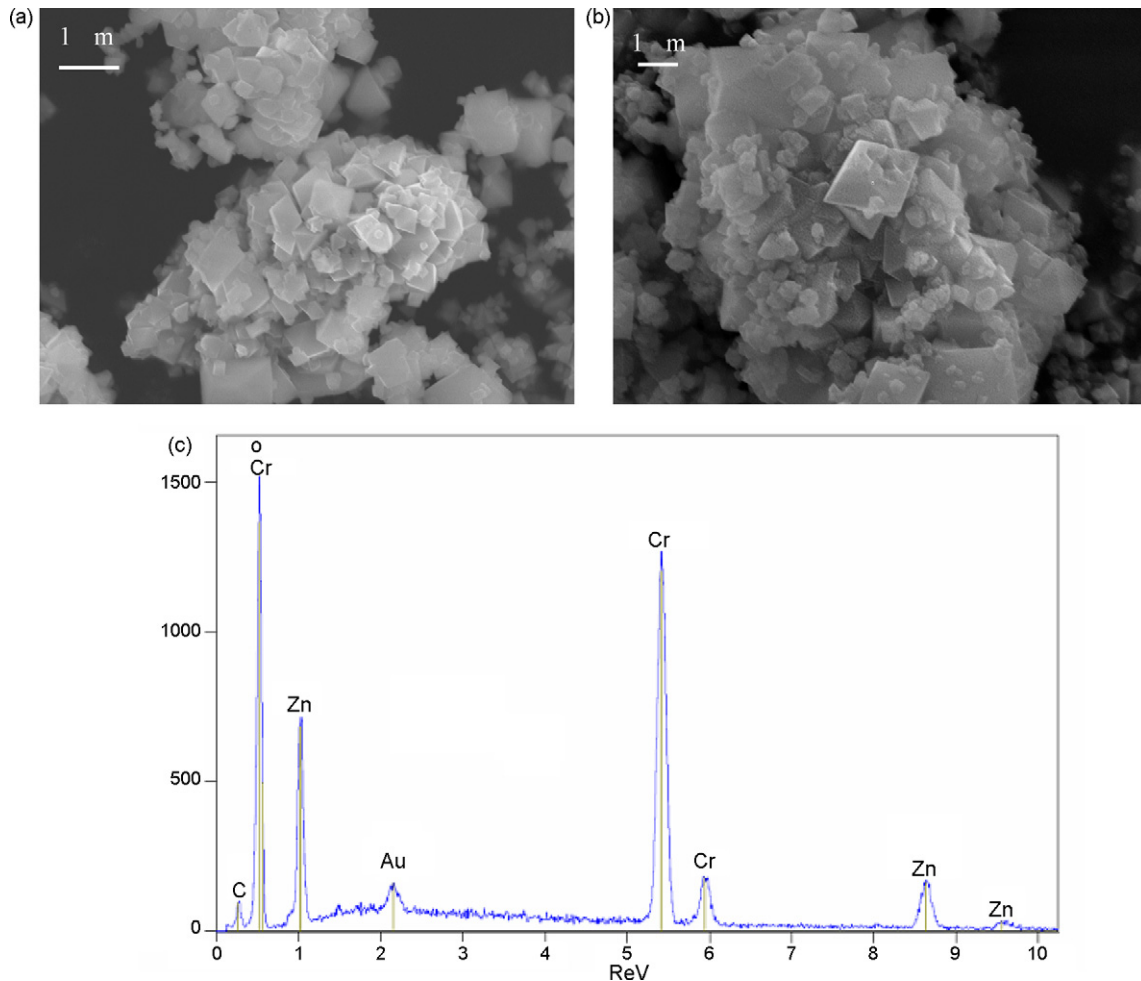


Fig. 3. Scanning electron micrograph images of (a) ZnCr_2O_4 and (b) $\text{ZnCr}_{1.85}\text{Fe}_{0.15}\text{O}_4$. (c) EDX pattern of ZnCr_2O_4 .

coordinated and occupied by trivalent cations (e.g., Al, Cr, Fe). Inverse spinel is characterized by the occupation of one of the B sites by the divalent cation and A site occupied by one of the trivalent cation. Zinc chromite crystallizes in normal spinel structure with the tetrahedral A site occupied by Zn^{2+} cations and the octahedral B site occupied by Cr^{3+} ions. Thus, the crystal structure of $ZnCr_2O_4$ comprises of ZnO_4 tetrahedra and CrO_6 octahedra. Zinc ferrite, Zn_2FeO_4 belongs to the same crystal structure, and a complete solid-solution between the two systems is reported.⁴¹

Oxide spinels have shown various interesting properties such as unusual magnetic properties and electrical conductivities. Generally, it is known that the cation distribution between A and B sites contributes to the magnetic properties and depends on the sample preparation process. Fe substitutes into Cr sites in CrO_6 octahedra. It is shown in literature that⁴¹ Fe substitution into $ZnCr_2O_4$ changes the electrical conductivity. We have been successful in doping Fe into ZCR by the above mentioned synthesis procedure as confirmed by the lattice parameter change from XRD peaks ($a = 8.2800 \text{ \AA}$, increase to 8.2920 \AA). The increase in lattice parameter is consistent with smaller Cr^{2+} (0.640 \AA) replacing larger Fe^{3+} (ionic radius 0.645 \AA).

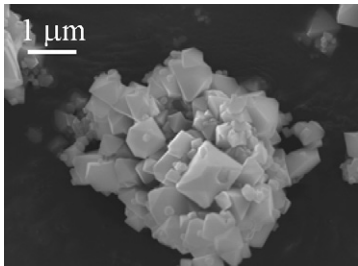
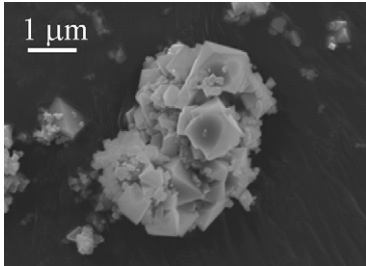
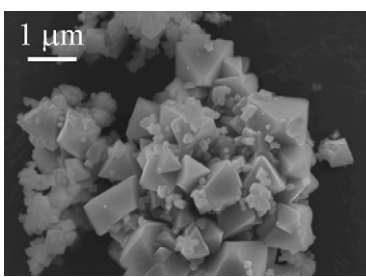
3.1. Microstructure of ZCR ceramic

The SEM image of the single-phase ZCR is shown in Fig. 3(a), which showed well-defined octahedron shaped morphology and uniform particle size. The valid surfaces for the cubic spinel lattice in the case of ZCR ceramic are (1 1 1), (2 2 0), (4 0 0), (3 1 1), (3 3 1), (4 2 2), and (5 1 1). Binks et al. has shown that the dominating surface is (1 1 1) on the basis of surface energy calculation, which leads to the regular octahedron geometry.⁴² Similar particle growth can be noticed for the ZCR sample synthesized by our procedure. The SEM morphology of Fe-doped ZCR is shown in Fig. 3(b), which confirms there was no change in the surface morphology of the ceramic particles. In addition, energy-dispersive X-ray (EDX), as shown in Fig. 3(c), confirmed the expected Zn to Cr ratio as well the phase-purity of the ceramic. In order to confirm the homogeneous distribution of the constituting elements, EDX analysis was performed on various particles having well defined morphology within different clusters. The results of the EDX along with corresponding SEM pictures are given in Table 2. From the EDX pattern, it is confirmed that the Zn to Cr ratio varied between 0.47 and 0.53 for ZCR ceramic particles within clusters, and the particles have well-defined octahedron morphology throughout. SEM and EDX results in conjunction with XRD results confirmed the chemical homogeneity of the ZCR samples synthesized by this procedure.

Fig. 4 shows the FTIR spectra of $ZnCr_2O_4$. The two high-frequency modes corresponding to peaks at 528 cm^{-1} and 635 cm^{-1} involve mainly the displacement of oxide anions relative to the chromium cations along the direction of the octahedral chains, and tentatively assigned to Cr–O stretching.¹²

Fig. 5 shows the XPS of $ZnCr_2O_4$. XPS provides valuable information concerning the elements in the near-surface region. Examination of the binding energies of the core-level

Table 2
EDX pattern with corresponding SEM pictures for different clusters of $ZnCr_2O_4$

Cluster	EDS	Morphology
1	$Zn_{0.8}Cr_{1.6}O_4$ $Zn_{1.1}Cr_{2.06}O_4$ $Zn_{0.8}Cr_{1.56}O_4$	
2	$Zn_{0.94}Cr_{1.76}O_4$ $Zn_{0.8}Cr_{1.58}O_4$ $Zn_{0.8}Cr_{1.56}O_4$ $Zn_{0.74}Cr_{1.56}O_4$	
3	$Zn_{1.06}Cr_2O_4$ $Zn_{0.82}Cr_{1.5}O_4$ $Zn_{0.8}Cr_{1.56}O_4$ $Zn_{1.0}Cr_{1.86}O_4$	

electronic states of the elements in the surface region provides qualitative, semi-quantitative, and chemical state information. Since the electron binding energy of an element differs from other elements, a full-scan spectrum was given for an overall understanding on the surface elemental constituents of the tested sample. In the spectra, we can see peaks corresponding to Zn 2p₁ (1045.2 eV), Zn 3s (135.0 eV), Zn 3p (91.6 eV), Zn 2p (1022.8 eV), Cr 3p (61.4 eV), Cr 2p (611.0 eV), and O 1s

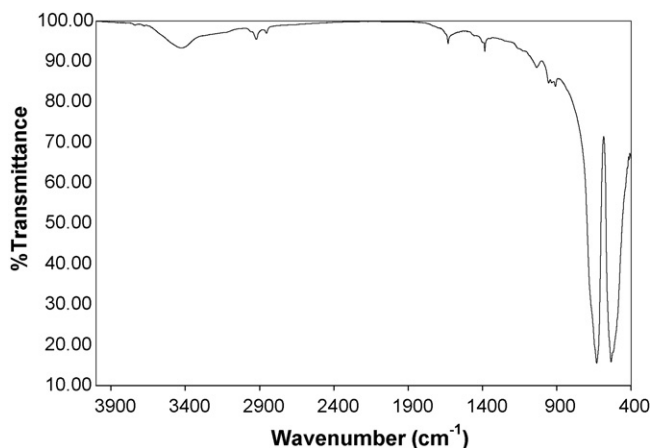
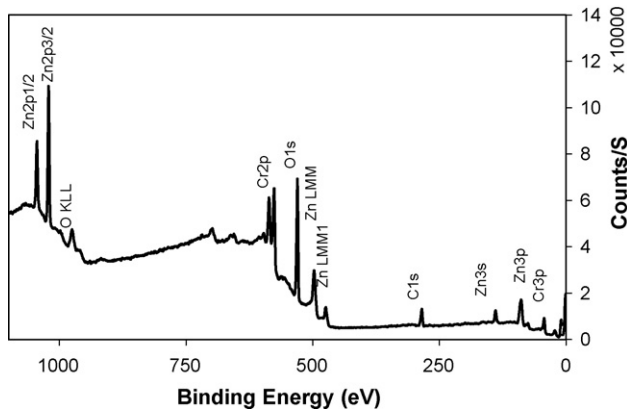


Fig. 4. FTIR spectra of $ZnCr_2O_4$.

Fig. 5. XPS data of ZnCr_2O_4 .

(531.6 eV). The C 1s peak at 284.8 eV is due to adventitious carbon present on the surface.

3.2. Physical properties of ZCR ceramic

Fig. 6 shows the diffuse reflectance spectra of the ZnCr_2O_4 samples in the UV–vis–NIR range. The diffuse reflectance data was used to calculate the absorption coefficient from the Kubelka–Munk (KM)⁴³ function defined as

$$F(R_\infty) = \frac{\alpha}{S} = \frac{(1 - R_\infty)^2}{2R}$$

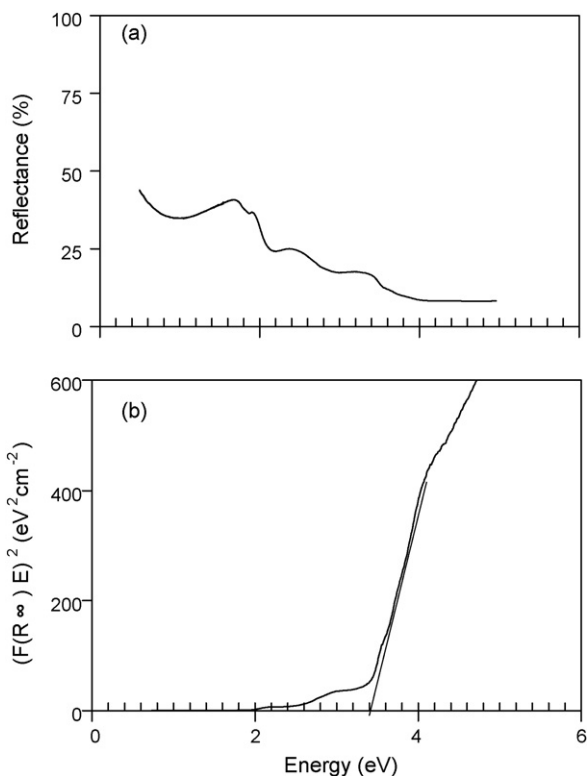


Fig. 6. (a) Diffuse reflectance spectra of ZnCr_2O_4 in the wavelength range of 250–2500 nm. (b) Plot of $F(R_\infty)$ vs. E (eV) for the estimation of the optical absorption edge energy.

Here “ α ” is the absorption coefficient, “ S ” is the scattering coefficient, and $F(R_\infty)$ is the KM function. For the diffused reflectance spectra, KM function can be used instead of “ α ” for the estimation of the optical absorption edge energy.⁴⁴ It was observed that a plot of $F(R_\infty)E$ versus E was linear near the edge for direct allowed transition ($\eta = 1/2$). The intercept of the line on abscissa ($F(R_\infty)E = 0$) gave the value of optical absorption edge energy to be 3.4 ± 0.2 eV. Fig. 6(b) shows the plot of the same.

ZnCr_2O_4 is a cubic spinel at room temperature with magnetic ions (Cr^{3+} , $s = 3/2$) at the B sites and is a typical example of the geometrically frustrated system. Temperature variation of magnetic susceptibility measurements confirmed that the ceramic material is paramagnetic above -173°C . Below this temperature, anti-ferromagnetic interaction develops. However, the geometry of the cubic lattice results in a frustrated spin system. A first-order anti-ferromagnetic transition with $T_N = -261.5^\circ\text{C}$, which relieves the frustration, is observed for these materials as reported earlier.^{45,46}

4. Conclusions

Single-phase, stoichiometric spinel ZnCr_2O_4 ceramic material was synthesized by a novel microwave-mediated metathesis route. The coexistence of NaCl and ZnCr_2O_4 phases in the as-prepared samples confirm the uniqueness of synthesizing such complex oxide material by simple, solid-state route. In addition, the method followed is cost-effective and less time consuming with a high yield. Fe doping into ZnCr_2O_4 confirms that this approach of synthesizing helps to (1) achieve the desired cation distribution in the ceramic material, (2) to fine tune the electrical and magnetic properties and (3) to tailor the material usage for many technological applications.

Acknowledgment

The authors would like to acknowledge Professor Allan Kirkpatrick, Head of Department of Mechanical Engineering, for his continued help, encouragement, and support.

References

- Martinho, H., Moreno, N. O., Sanjurjo, J. A., Rettori, C., Garcia-Adeva, A. J., Huber, D. L. *et al.*, Magnetic properties of the frustrated anti-ferromagnetic spinel ZnCr_2O_4 and the spin-glass $\text{Zn}_{1-x}\text{Cd}_x\text{Cr}_2\text{O}_4$ ($x = 0.05, 0.10$). *Phys. Rev. B*, 2001, **64**, 1–6.
- Zerr, A., Miede, G., Serghiu, G., Schwarz, M., Kroke, E., Riedel, R. *et al.*, Synthesis of cubic silicon nitride. *Nature*, 1999, **400**, 340–342.
- Kim, B. N., Hiraga, K., Morita, K. and Sakka, Y., A high-strain-rate superplastic ceramic. *Nature*, 2001, **413**, 288–291.
- Gabr, R. M., Girgis, M. M. and Elawad, A. M., Formation, conductivity and activity of zinc chromite catalyst. *Mater. Chem. Phys.*, 1992, **30**, 169–177.
- El-Sharkawy, E. A., Textural, structural and catalytic properties of $\text{ZnCr}_2\text{O}_4\text{-Al}_2\text{O}_3$ ternary solid catalysts. *Adsorpt. Sci. Technol.*, 1998, **16**, 193–216.
- Epling, W. S., Hoflund, G. B. and Minahan, D. M., Reaction and surface characterization study of higher alcohol synthesis catalysts. VII. Cs- and Pd-promoted 1:1 Zn/Cr spinel. *J. Catal.*, 1998, **175**, 175–184.
- Bayhan, M., Hashemi, T. and Brinkman, A. W., Sintering and humidity-sensitive behavior of the $\text{ZnCr}_2\text{O}_4\text{-K}_2\text{CrO}_4$ ceramic system. *J. Mater. Sci.*, 1997, **32**, 6619–6623.

8. Golonka, L. J., Licznarski, B. W., Nitsch, K. and Teterycz, H., Thick-film humidity sensors. *Meas. Sci. Technol.*, 1997, **8**, 92–98.
9. Pokhrel, S., Jeyaraj, B. and Nagaraja, K. S., Humidity-sensing properties of $\text{ZnCr}_2\text{O}_4\text{-ZnO}$ composites. *Mater. Lett.*, 2003, **4378**, 1–6.
10. Lee, S.-H., Broholm, C., Ratcliff, W., Gasparovic, G., Huang, Q., Kim, T. H. *et al.*, Emergent excitations in a geometrically frustrated magnet. *Nature*, 2002, **418**(6900), 856–858.
11. Jo, Y., Park, J.-G., Kim, H. C., Ratcliff, W. and Cheong, S.-W., Pressure-dependent magnetic properties of geometrically frustrated ZnCr_2O_4 . *Phys. Rev. B: Condens. Matter Mater. Phys.*, 2005, **72**(18), 184421/1–184421/5.
12. Marinkovic, Z. V., Mancic, L., Vulic, P. and Milosevic, O., Microstructural characterization of mechanically activated $\text{ZnO-Cr}_2\text{O}_3$ system. *J. Eur. Ceram. Soc.*, 2005, **25**, 2081–2084.
13. Marinkovic, Z. V., Mancic, L., Vulic, P. and Milosevic, O., The influence of mechanical activation on the stoichiometry and defect structure of a sintered $\text{ZnO-Cr}_2\text{O}_3$ system. *Mater. Sci. Forum*, 2004, **453/454**, 423–428.
14. Levy, D., Diella, V., Pavese, A., Dapiaggi, M. and Sani, A., P - V equation of state, thermal expansion, and P - T stability of synthetic (ZnCr_2O_4 spinel). *Am. Mineral.*, 2005, **90**, 1157–1162.
15. Marinkovic, Z. V., Romcevic, N. and Stojanovic, B., Spectroscopic study of spinel ZnCr_2O_4 obtained from mechanically activated $\text{ZnO-Cr}_2\text{O}_3$ mixtures. *J. Eur. Ceram. Soc.*, 2006, **27**, 903–907.
16. Wang, Z., Lazor, P., Saxena, S. K. and Artioli, G., High-pressure Raman spectroscopic study of spinel (ZnCr_2O_4). *J. Solid State Chem.*, 2002, **165**, 165–170.
17. Niu, X., Du, W. and Du, W., Preparation and gas sensing properties of ZnM_2O_4 ($M = \text{Fe, Co, Cr}$). *Sens. Actuators B*, 2004, **99**, 405–409.
18. Chandran, R. G. and Patil, K. C., A rapid method to prepare crystalline fine particle chromite powders. *Mater. Lett.*, 1992, **12**(6), 437–441.
19. Adak, A. K., Pathak, A. and Pramanik, P., Polyvinyl alcohol evaporation method for preparation of submicron chromite powders. *Br. Ceram. Trans.*, 1999, **98**, 200–203.
20. Shrout, T. R., Adair, J. H. and Swartz, S., Chemical route to ultrafine zinc chromite (ZnCr_2O_4) and cadmium chromite (CdCr_2O_4) spinel powders. *Ceram. Trans.*, 1990, **12**, 155–162.
21. Marinkovic, Z. V., Mancic, L., Maric, R. and Milosevic, O., Preparation of nanostructured Zn-Cr-O spinel powders by ultrasonic spray pyrolysis. *J. Eur. Ceram. Soc.*, 2001, **21**, 2051–2055.
22. Bonneau, P. R., Jarvis, R. F. and Kaner, R. B., Rapid solid-state synthesis of materials from molybdenum disulfide to refractories. *Nature*, 1991, **349**, 510–512.
23. Parhi, P., Ramanan, A. and Ray, A. R., A convenient route for the synthesis of hydroxyapatite through a novel microwave-mediated metathesis reaction. *Mater. Lett.*, 2004, **58**, 3610–3612.
24. Parhi, P., Ramanan, A. and Ray, A. R., Synthesis of nano-sized alkaline-earth hydroxyapatites through microwave assisted metathesis route. *Mater. Lett.*, 2006, **60**, 218–221.
25. Mandal, T. K. and Gopalakrishnan, J., New route to ordered double perovskites: synthesis of rock salt oxides, Li_4MWO_6 , and their transformation to Sr_2MWO_6 ($M = \text{Mg, Mn, Fe, Ni}$) via metathesis. *Chem. Mater.*, 2005, **17**, 2310–2316.
26. Gopalakrishnan, J., Sivakumar, T., Ramesha, K., Thangadurai, V. and Subbanna, G. N., Transformations of Ruddlesden-Popper oxides to new layered perovskite oxides by metathesis reactions. *J. Am. Chem. Soc.*, 2000, **122**, 6237–6241.
27. Nartowski, A. M., Parkin, I. P., MacKenzie, M., Craven, A. J. and Macleod, I., Solid-state metathesis routes to transition metal carbides. *J. Mater. Chem.*, 1999, **9**, 1275–1281.
28. Rao, L., Gillan, E. G. and Kaner, R. B., Rapid synthesis of transition metal borides by solid-state metathesis. *J. Mater. Res.*, 1995, **10**, 353–361.
29. Treece, R. E., Conklin, J. A. and Kaner, R. B., Metathetical synthesis of binary and ternary anti-ferromagnetic gadolinium pnictides (P, As, and Sb). *Inorg. Chem.*, 1994, **33**, 5107–5701.
30. Mingos, D. and Michael, P., Microwave syntheses of inorganic materials. *Adv. Mater.*, 1993, **5**, 857–859.
31. Vaidhyanathan, B., Ganguli, M. and Rao, K. J., Fast solid-state synthesis of metal vanadates and chalcogenides using microwave irradiation. *Mater. Res. Bull.*, 1995, **30**, 1173–1177.
32. Bhunia, S. and Bose, D. N., Microwave synthesis, single crystal growth and characterization of ZnTe . *J. Cryst. Growth*, 1998, **186**, 535–542.
33. Ramesh, P. D. and Rao, K. J., Microwave-assisted synthesis of aluminum nitride. *Adv. Mater.*, 1995, **7**, 177–179.
34. Vaidhyanathan, B. and Rao, K. J., Synthesis of Ti, Ga, and V nitrides: microwave assisted carbothermal reduction and nitridation. *Chem. Mater.*, 1997, **9**, 1196–1200.
35. Vaidhyanathan, B., Raizada, P. and Rao, K. J., Microwave assisted fast solid-state synthesis of niobates and titanates. *J. Mater. Sci. Lett.*, 1997, **16**, 2022–2025.
36. Vaidhyanathan, B. and Rao, K. J., Microwave assisted synthesis of technologically important transition metal silicides. *J. Mater. Res.*, 1997, **12**, 3225–3229.
37. Kosslick, H., Zutowa, H. L., Lohse, U., Landmesser, H., Fricke, R. and Caro, J., Microwave processing of zeolites. *Ceram. Trans.*, 1997, **80**, 523–537.
38. Wagner, C. D., Naumkin, A. V., Kraut-Vass, A., Allison, J. W., Powel, C. J. and Rumbles, J. R., NIST X-ray Photoelectron Spectroscopy Database. 2000.
39. JCPDS Card No. 05-0628, ICDD, PCPDFWIN v.2.1, JCPDS-International Centre for Diffraction Data. 2000.
40. JCPDS Card No. 73-1962, ICDD, PCPDFWIN v.2.1, JCPDS-International Centre for Diffraction Data. 2000.
41. Yoon, S. J., Lee, S. H., Kim, K. H. and Ahn, K. S., Electrical and magnetic properties of spinel $\text{ZnCr}_{2-x}\text{Fe}_x\text{O}_4$ ($0 \leq x \leq 1.0$). *Mater. Chem. Phys.*, 2002, **73**, 330–334.
42. Binks, D. J., Grimes, R. W., Rohl, A. L. and Gay, D. H., Morphology and structure of ZnCr_2O_4 spinel crystallites. *J. Mater. Sci.*, 1996, **31**, 1151–1156.
43. Kortum, G., *Reflectance Spectroscopy Principles, Methods, Applications*. Springer-Verlag, New York, 1969.
44. Barton, D. G., Shtein, M., Wilson, R. D., Soled, S. L. and Iglesia, E., Structure and electronic properties of solid acids based on tungsten oxide nanostructures. *J. Phys. Chem. B*, 1999, **103**, 630–640.
45. Kino, Y. and Luethi, B., Magnetic and elastic properties of zinc chromite. *Solid State Commun.*, 1971, **9**, 805–808.
46. Kagomiyaa, I., Toki, M., Kohn, K., Hata, Y., Kita, E. and Siratori, K., Magnetic clusters in three dimensional spin frustrated system ZnCr_2O_4 . *J. Magn. Mater.*, 2004, **272–276**, e1031–e1032.